

**Off-axis emission of electrons by discharge of a low-inductance vacuum spark**P. S. Antsiferov<sup>1,2,\*</sup>, L. A. Dorokhin,<sup>1</sup> and D. Spinov<sup>3</sup><sup>1</sup>*Institute of Spectroscopy of Russian Academy of Sciences, Fizicheskaya str. 5, 108840 Troitsk, Moscow, Russia*<sup>2</sup>*HSE University, Physical faculty, Myasnitskaya str. 20, 101000, Moscow, Russia*<sup>3</sup>*Moscow Institute of Physics and Technology, Institutsky line 9, 141700 Dolgoprudny, Russia*

(Received 19 January 2023; accepted 14 November 2023; published 6 December 2023)

The article presents the results of the study of electrons, emitted by the plasma of a low-inductance vacuum spark. It was found that a 50-kA discharge with a 3.4- $\mu$ s period of current oscillations produces electrons with the energy higher than 100 keV, which leave the discharge plasma in the direction perpendicular to the discharge axis. The electrons have an energy spectrum close to monoenergetic. They appear after the first quarter period of discharge current oscillations and are emitted during about 1  $\mu$ s. So, the origin of the electrons has no relation to the process of plasma pinching. The time behavior of the electron energy was studied. It gradually diminishes from a value of about 100 keV just after the maximum of the discharge current down to about 10 keV after reversal of the current direction. This phenomenon points out the redistribution of the discharge current, resulting in the disappearance of the magnetic field on the line of sight perpendicular to the discharge axis.

DOI: [10.1103/PhysRevE.108.065206](https://doi.org/10.1103/PhysRevE.108.065206)**I. INTRODUCTION**

The appearance of accelerated electrons in high current discharges had been noticed already in first experiments, aimed on the creation of hot plasma [1]. This phenomenon has been found in many types of discharges, for example in plasma focus [2,3], Z pinch [4], and low-inductance vacuum spark [5,6]. Review [7] describes the physical picture of the low-inductance vacuum spark (LIVS) discharge (vacuum discharge with maximal current about 100 kA and period of oscillations in the microsecond scale), where the acceleration of electrons reveals itself in the generation of hard x rays [8,9]. The mechanism of the electrons acceleration here is closely connected with deep pinching of the discharge plasma and generation of the overvoltage due to the jump of plasma Ohmic resistance [10,11]. So the experimental methods of the study of high-energy electrons, generated in LIVS, involved mostly the study of electron emission along the discharge axis [12], because the high value of the magnetic field of the discharge current (about several tesla) gives no chance for electrons to leave the discharge plasma perpendicular to the discharge axis at the moment of pinching. In contrast to that, the present work reports the results of the study of electrons, generated by LIVS in direction perpendicular to the discharge axis. These electrons appear after the phase of compression and definitely have no relation to the process of the plasma pinching. They are produced in a wide range of charging voltages and with different materials of the anode, which define the chemical composition of the discharge plasma. The problem of the mechanism of these electrons generation is still open.

The LIVS discharge is a well-studied physical object, and it was difficult to predict the detection of electrons in the side-on direction. The usage of the microchannel plate as a detector of images of the pinhole camera was the main point, which made it possible to find it. Another reason of the absence of the information about this phenomenon in the literature can be connected with the geometry of radial emission of electrons—they do not hit the anode but spread out over the inner surface of the discharge camera. That makes the brightness of the corresponding hard x-ray emission much less. Together with smooth time dependence (see below) it makes it more difficult to detect hard x rays, caused by radial emitted electrons, in comparison with the short, bright pulse of hard x rays produced during fast pinching.

**II. EXPERIMENT**

The present experiments have been done with LIVS, which included the main capacitor  $C = 3 \mu\text{F}$  (charging voltage 6–12 kV) and a discharge unit with a triggering arrangement (see Fig. 1). The period of the oscillations in the discharge circuit is 3.4  $\mu$ s and the first maximum of current is 50 kA. The residual pressure in the system was about  $10^{-2}$  Pa. The discharge is triggered by means of the high-voltage pulse, generated in a separate circuit. This circuit contains the 0.1- $\mu$ F capacitor charged up to 10 kV. The trigger electrode has been embodied in the cathode through the insulating pipe. The main experimental tools are the pinhole camera and the microchannel plate (MCP) detector [13], working in the imaging mode. The MCP detector construction is an assembly of a MCP and a phosphor screen. The geometrical magnification of the pinhole camera is 3. The plasma-detector distance is 200 mm. The sensitive part of the MCP is exposed by the pinhole camera image, which contains the anode-cathode gap of the discharge diode (see Fig. 1). The

\*Corresponding author: Ants@isan.troitsk.ru

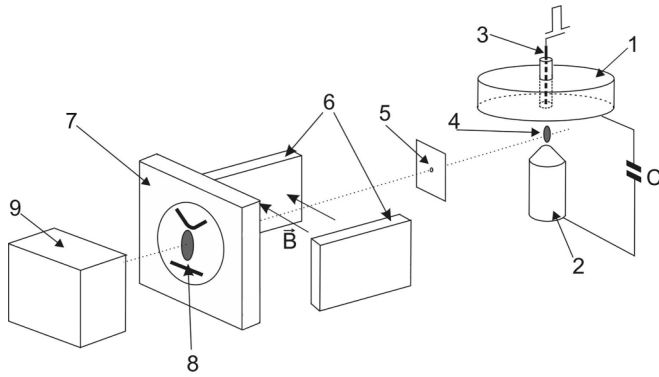


FIG. 1. The general scheme of the experimental setup. 1,2: the discharge electrodes, cathode, and anode; 3: the trigger electrode; 4: the discharge plasma; 5: the image-forming aperture; 6: permanent magnets; 7: microchannel plate detector; 8: the image of the discharge gap; 9: the digital camera.

image of plasma is taken from the phosphor screen by means of a digital camera. The detector is sensitive to both soft x-ray radiation and charged particles flux [14]. The detector has been gated by means of a 10-ns pulse, synchronized with the discharge current. There was a possibility to apply a magnetic field of the order of  $10^{-3}$  T to the volume of the pinhole camera by means of the permanent magnets (see Fig. 1).

Typical pinhole images, obtained without application of a magnetic field, are shown in Fig. 2 together with the discharge current curve. The current curve has been obtained by means of a magnetic probe. The images of discharges, presented in Fig. 2, have been produced with the usage of an Al anode. The triggering time is given with respect to the moment of the beginning of the discharge current. The first quarter period of the discharge current oscillations gives rise to the plasma column, connecting the anode and the cathode of the discharge diode. It is possible to catch the frames with pinching of the discharge column. The pinhole camera images at time delays  $t > 1200$  ns from the beginning of the discharge reveal a spot feature, that exists in the discharge even when the discharge current reverses its direction (see Fig. 2). This feature is the object of the investigations described in the present article.

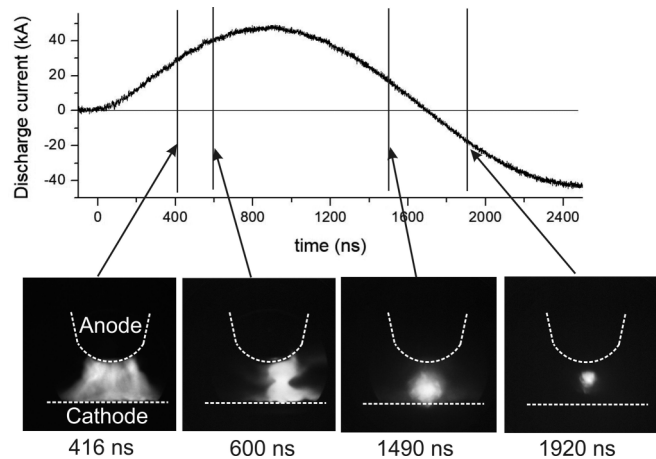


FIG. 2. Current curve (upper image) and a series of pinhole images (lower line of images), obtained at different time delays with respect to the start of the discharge current.

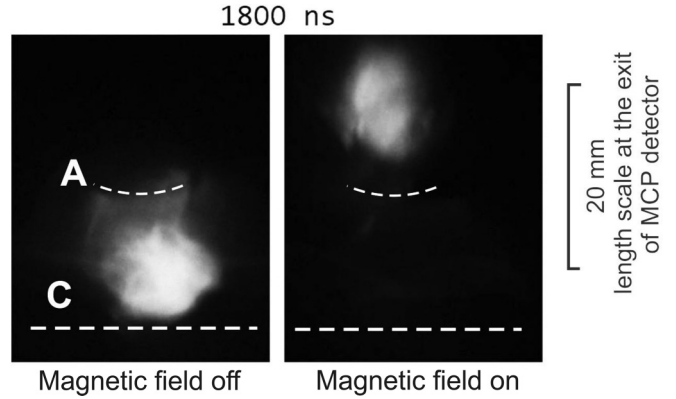


FIG. 3. The influence of the magnetic field upon the position of the spot feature in the discharge.

III. EXPERIMENTAL RESULTS

The main phenomenon is the influence of the magnetic field upon the position of the mentioned spot feature. Figure 3 presents its displacement by the application of a magnetic field about 0.001 T at a length of about 20 cm (see Fig. 1). The images were obtained with the usage of a Mo anode. The direction of the displacement shows that the image is formed by the electrons. The displaced spot still remains a compact feature; this indicates that the energy spectrum of the detected electrons is close to monoenergetic. The particular form of the displaced spot differs from discharge to discharge, but every time it corresponds to the energy spectrum of electrons with a definite maximum at a certain energy. So we will refer to the generated electrons as the electron beam in the following text. The magnetic field profile along the axis of the pinhole camera has been measured, which made it possible to calibrate the displacement of the electron spot at the image by the field application in terms of the energy of the electrons via numerical tracing of the electron trajectories. The point of the spot, corresponding to the position of the maximum of the brightness at the image was considered as a beam center position for the calculation of the energy of the electron beam. The application of the same magnetic field behind the discharge chamber, on the opposite side with respect to the pinhole camera, caused no influence on the pinhole camera images. So, we can be sure that the magnetic field in the volume of the pinhole camera does not disturb the discharge.

The results of the measurement of the electron beam energy dependent on the time delay with respect to the start of the discharge current are given in Figs. 4 and 5. Figure 4 presents the results at different charging voltages for the discharge diode with the Mo anode. Each point on the graph is the result of the averaging of about ten measurements, and the error bars correspond to  $3\sigma$ . Figure 4 shows that the electron beam energy exceeds 100 keV at time delays between 1200 and 1400 ns. One can see that the properties of the electron beam do not depend on the charging voltage within the range 6–12 kV. Figure 5 demonstrates the dependence of the electron beam properties on the material of the anode at charging voltage 12 kV. Most likely the reason for the difference in the energy of the electron beam for different anode materials is connected to the different density of plasma, because the rate

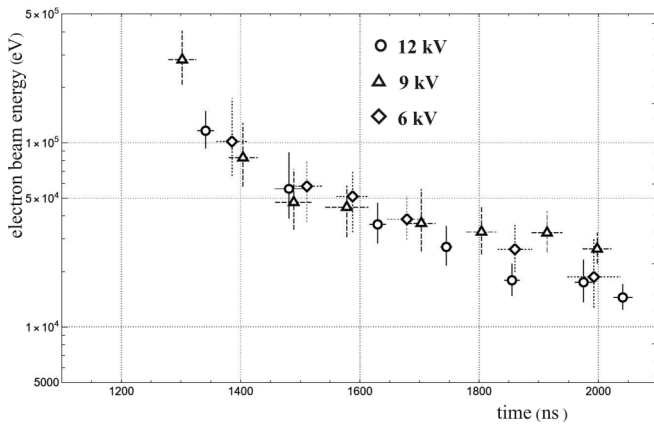


FIG. 4. The results of the measurement of the electron beam energy at different charging voltages. The material of the anode electrode is Mo.

of the anode erosion at the definite discharge current depends upon the anode material.

The present results show that the generation of the electron beam takes place at time moments considerably later than the time of the plasma pinching. The pinching takes place within the first quarter period of the discharge current oscillations, and the electrons appear at the second and third quarter periods. The electron beam appears even when the Pb anode is used in the vacuum diode, although the pinhole camera images show that the discharges with the Pb anode reveal no pinching at all in our setup. The generation of the electron beam takes place during a considerable time interval, about 1  $\mu$ s, while the electrons originated in pinches usually are short pulses. So, we conclude that the electrons under study are of a quite different nature in comparison with the electrons appearing by pinching.

**IV. THE RESULTS OF MEASUREMENTS WITH MCP IN CURRENT MODE**

The detailed information about the time behavior of the accelerated electrons can be obtained with the usage of a MCP in the current regime (see Fig 6). This arrangement implies dc bias of the MCP in the range 600–800 V. The sensitive

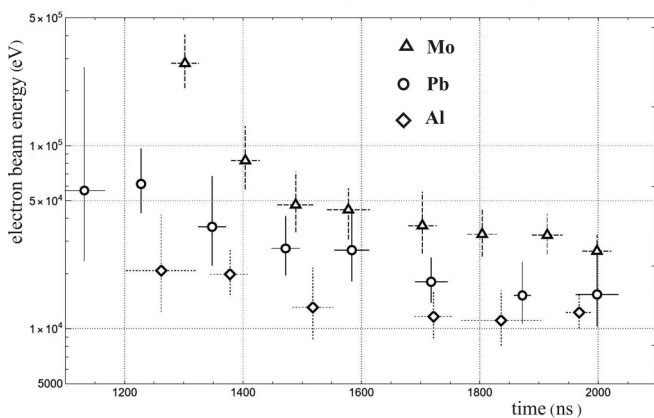


FIG. 5. The results of the measurement of the electron beam energy for different materials of the anode. The charging voltage is 12 kV.

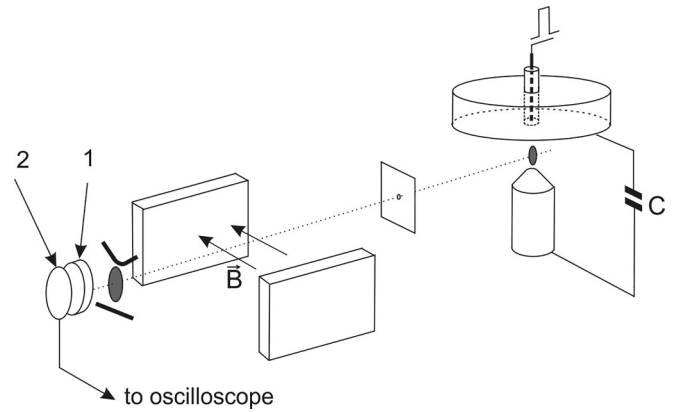


FIG. 6. The scheme of the experiment with the usage of a MCP in the current regime. 1: MCP; 2: current collector electrode.

part of the MCP is exposed by part of pinhole camera image, corresponding to the anode-cathode gap of the discharge diode (see Fig. 6). The signal from the collector electrode has been analyzed by means of a digital oscilloscope. More detailed information about this mode of the MCP detector is given in [15]. Typical results for the discharge diode with Al and Mo anodes are given in Figs. 7 and 8. The signal from the collector electrode, loaded on 50  $\Omega$ , is given together with the current curve. Irreproducible pulses during the first quarter of discharge current oscillations correspond to extreme ultraviolet radiation emitted by pinching plasma. A wide pulse after 1200 ns is the electron beam signal. The application of the magnetic field results in its disappearance. The electrons have been emitted even after the reversal of the direction of the discharge current. One can see that the time behavior of the total electron beam current is smooth and does not contain any pronounced time structure, at least down to a timescale of about several tens of nanoseconds.

The results presented in Figs. 7(b) and 8(b) can be used for the estimation of the total electron beam current. The output current of the MCP detector in the current regime produces a voltage of about 1 V on a 50- $\Omega$  load, that corresponds to the

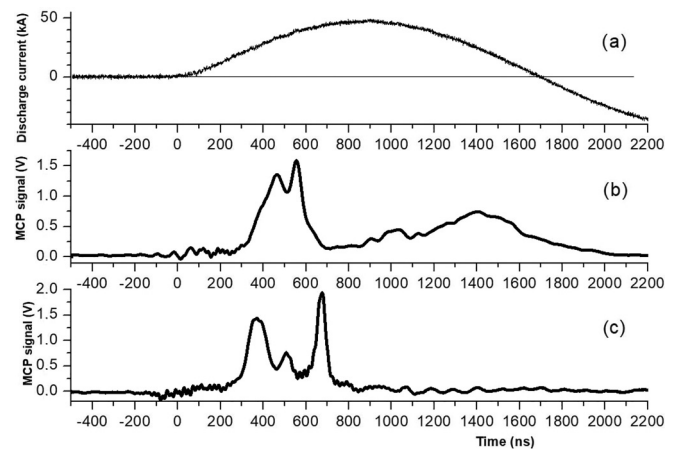


FIG. 7. Time behavior of the MCP signal for the discharge with the Al anode. (a) Discharge current curve; (b) MCP signal without magnetic field in the pinhole camera volume; (c) MCP signal with the magnetic field applied to the volume of the pinhole camera.

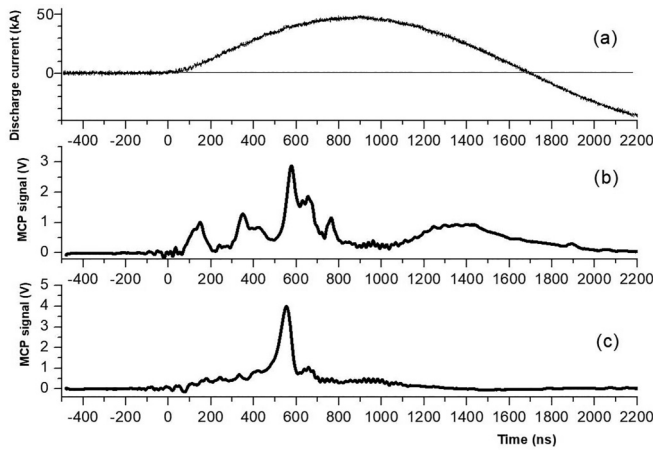


FIG. 8. Time behavior of the MCP signal for the discharge with the Mo anode. (a) Discharge current curve; (b) MCP signal without the magnetic field in the pinhole camera volume; (c) MCP signal with the magnetic field applied to the volume of the pinhole camera.

output current 0.02 A. The maximal gain of the MCP is about  $10^4$ ; this corresponds to the current at the entrance of the MCP of about  $2 \times 10^{-6}$  A. The quantum efficiency of the MCP for the electrons in our range of energies is within 10%–20%, so the value of the electron beam current at the entrance of the MCP can be estimated as  $10^{-5}$  A. The image-forming aperture in the pinhole camera defines the solid angle of the electron beam (0.1 mm on the distance 50 mm). Neglecting the angle dependence of the properties of the electron beam, we get the estimation of the peak value of the total electron beam current in  $4\pi$  sr as about 30 A.

V. DISCUSSION

The emission of electrons by discharge plasma in the direction perpendicular to the discharge axis means that there is no magnetic field on the line of sight of the pinhole camera. The maximal energy of the electron beam (about 100 keV) corresponds to the time delay with respect to the beginning of the discharge at about 1400 ns. At that moment the discharge current is 25 kA (see Fig. 1). Would this current go through the plasma between the anode and the cathode, the estimation of the magnetic field at the radius equal to the radius of the anode ( $r = 1.5$  mm) gives  $B = \mu_0 \frac{I}{2\pi r} = 3.3T$ . The value of the Larmor radius for 100-keV electrons at such  $B$  is about 0.5 mm and they have no possibility to directly leave the plasma or to form a compact image at the MCP detector. The situation is even more serious at a time delay of about 2000 ns, where at the same value of discharge current the energy of the electron beam is only about 10 keV. This, in turn, means that after about 1200 ns from the beginning of the discharge the current has been substantially redistributed (see Fig. 9). The current must flow not through the anode-cathode gap, but between the anode and the discharge chamber inner wall, which has the same potential as the cathode. Such redistribution matches the fact of weak sensitivity of the electron beam properties on the charging voltage, because in this case the electron emission takes place without any current flowing through the plasma. The absence of the influence of the

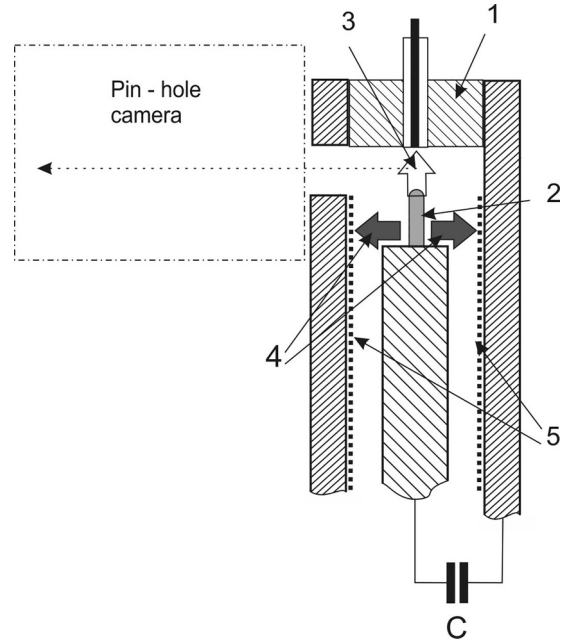


FIG. 9. The scheme of the redistribution of the discharge current. 1: cathode; 2: anode; 3: discharge current up to 1200 ns from the beginning of the discharge; 4, discharge current after 1200 ns from the beginning of the discharge; 5: the insertion of the cylindrical insulator into the discharge chamber prevents the appearance of the accelerated electrons.

discharge current value upon the electron beam also matches the results with the MCP detector in the current regime; the electron beam signal in Figs. 7 and 8 does not “feel” in any way the moment of zero crossing by the discharge current.

The physical picture given above can be checked also by preventing the discharge current redistribution. For that an insulating cylinder has been inserted along the inner wall of the discharge chamber (position 5 in Fig. 9). The images with and without application of a magnetic field are shown in Fig. 10 (Mo anode). Figure 10 should be compared with Fig. 3. The cloudlike feature between the anode and the cathode now is not sensitive to the application of a magnetic field. So, the visible image most likely has been formed by the radiation of the plasma, and accelerated electrons do not appear. This

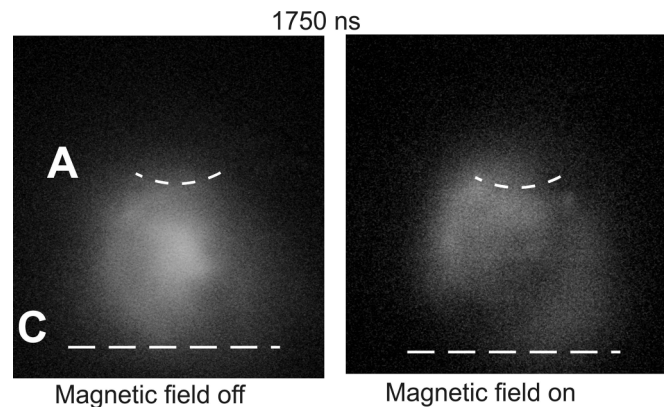


FIG. 10. The pinhole camera image of the discharge gap with the insulator 5 (see Fig. 9) inserted into the discharge chamber.

fact corresponds to the proposed mechanism of the discharge current redistribution.

One could hardly imagine the existence of the potential difference of about 100 kV in the radial direction of the decaying plasma during a time of about 1  $\mu$ s. A plausible mechanism of electron acceleration can be connected with the radial oscillations of the plasma electrons, which become possible after the redistribution of the discharge current. The magnetic field of the discharge current before 1200 ns influences the radial motion of the plasma electrons, limiting their displacement. The appearance of the running radial waves of electron density can result in electron acceleration, as takes place in the process of wakefield acceleration [16]. The source of the energy of radial oscillations could be connected with the expansion of the decaying discharge plasma. The physical mechanism of the generation of radial running waves can be connected with the diminishment of plasma density in the radial direction, resulting in the diminishment of plasma frequency. This should produce a phase modulation of radial oscillations. Such modulation can be responsible for the appearance of the running radial waves of electron density, which can produce the acceleration of the electrons.

## VI. CONCLUSION

The present work reports the results of the study of electrons emission by the LIVS discharge with a maximal

discharge current of about 50 kA. The emission has been detected in the direction perpendicular to the discharge axis, which hints at the absence of a magnetic field around the discharge plasma. The electron beam energy spectrum is close to monochromatic. The electrons are emitted during a comparatively long time—about 1  $\mu$ s. The time behavior of the electrons energy has been investigated. This energy gradually decreases from the value of about 100 keV at time delay 1200 ns from the beginning of the discharge to the value of about 10 keV at time delays more than 2000 ns. The origin of the emitted electron beam is not connected with plasma pinching. A possible mechanism is the electrons acceleration by the radial running waves of electron density. The study of the electron density at the plasma decay stage can clarify the mechanism of the electrons acceleration. The use of interferometry seems to be adequate for the density investigations, and it is included in the future working plans of the authors. The understanding of the mechanism of the electrons generation in the LIVS discharge can be useful for the elaboration of very simple sources of 100-keV electrons.

## ACKNOWLEDGMENT

This research is funded by the research Project No. FFUU-2022-0005 of the Institute of Spectroscopy of the Russian Academy of Sciences.

- 
- [1] L. A. Artsimovich, *Controlled Thermonuclear Reactions* (Oliver & Boyd, New York, 1964).
  - [2] T. Yamamoto, K. Shimoda, and K. Hirano, *J. Appl. Phys.* **24**, 324 (1985).
  - [3] J. R. Smith, C. M. Luo, M. J. Rhee, and R. F. Schneider, *Phys. Fluids* **28**, 2305 (1985).
  - [4] D. R. Kania and L. A. Jones, *Phys. Rev. Lett.* **53**, 166 (1984).
  - [5] J. Fukai and E. J. Clothiaux, *Phys. Rev. Lett.* **34**, 863 (1975).
  - [6] H. S. Uhm and T. N. Lee, *Phys. Rev. A* **40**, 3915 (1989).
  - [7] K. N. Koshelev and N. R. Pereira, *J. Appl. Phys.* **69**, R21 (1991).
  - [8] T. N. Lee and R. C. Elton, *Phys. Rev. A* **3**, 865 (1971).
  - [9] O. A. Bashutin and A. S. Savjolov, *Plasma Phys. Rep.* **42**, 347 (2016).
  - [10] Y. S. Choi, T. N. Lee, and U. S. Uhm, *Phys. Lett. A* **189**, 80 (1994).
  - [11] A. N. Dolgov and V. V. Vikhrev, *Plasma Phys. Rep.* **31**, 259 (2005).
  - [12] O. A. Bashutin, I. G. Grigoryeva, A. N. Korf, A. S. Savelov, and G. Kh. Salakhutdinov, *Phys. At. Nucl.* **83**, 1445 (2020).
  - [13] D. Shan, T. Yanagidaira, K. Shimoda, and K. Hirano, *Rev. Sci. Instrum.* **70**, 1688 (1999).
  - [14] M. Galanti, R. Gott, and F. Renaud, *Rev. Sci. Instrum.* **42**, 1818 (1971).
  - [15] P. S. Antsiferov, L. A. Dorokhin, and K. N. Koshelev, *J. Appl. Phys.* **107**, 103306 (2010).
  - [16] T. Tajima and J. M. Dawson, *Phys. Rev. Lett.* **43**, 267 (1979).